ORIGINAL PAPER

# Novel carrageenan-based hydrogel nanocomposites containing laponite RD and their application to remove cationic dye

**Gholam Reza Mahdavinia · Abdolhossein Massoudi · Ali Baghban · Bakhshali Massoumi**

**Abstract** Novel hydrogel nanocomposites were synthesized by solution polymerization of acrylamide in the presence of carrageenan biopolymer and laponite RD clay. Laponite was used as an inorganic cross-linker. Ammonium persulfate was applied as an initiator. The structure and morphology of the nanocomposites were investigated using XRD, scanning electron microscopy, and transition electron microscopy techniques. The influence of both laponite nanoclay and the carrageenan content on the swelling degree of nanocomposites was studied and it was found that all nanocomposites containing carrageenan component have a high swelling degree compared to a nanocomposite without carrageenan. The obtained nanocomposites were examined to remove a cationic crystal violet (CV) dye from water. The effect of carrageenan and clay contents on the speed of dye adsorption revealed that while the rate of dye adsorption is enhanced by increasing the clay content, it was depressed as the carrageenan content increased in nanocomposite composition. The results showed that the pseudo-second-order adsorption kinetic was predominant in adsorption of CV onto nanocomposites. The experimental equilibrated adsorption capacity of nanocomposites was analyzed using Freundlich and Langmuir isotherm models. The results indicated that the experimental data fit the Langmuir isotherm best. Maximum adsorption capacity was obtained for carrageenan-free nanocomposite with 79.8 mg g$^{-1}$ of adsorbed CV onto nanocomposite.

**Keywords** Carrageenan · Nanocomposite · Hydrogel · Laponite · Removal

## Introduction

Hydrogels are hydrophilic polymer networks that can absorb a large amount of water from aqueous solutions without being dissolved. These networks can be synthesized through chemical or physical cross-linking. In chemical cross-linking, an appropriate organic cross-linker such as methylenebisacrylamide is usually used for polymer chains to connect each other by covalent bonds. In contrast, the physical cross-linking takes place by ionic or hydrogen bonds [1].

Recently, nanocomposite hydrogels have been synthesized using different nanoclays [2]. Among them, the hydrogels containing laponite nanoclay have attracted the attention of researchers. Haraguchi et al. [3, 4] have reported the synthesis of hydrogel nanocomposites without using organic cross-linkers. They have used laponite nanoclay as multifunctional cross-linker. The cross-linking mainly occurs in the presence of monomers containing the amide group, whereby the ionic and polar interactions at the clay–polymer interface would lead to physical cross-linking. In fact, by applying laponite nanoclay into a hydrogel composition, there would be physical cross-linking facilitated without any need of chemical cross-linkers to achieve sufficient improvements in physical and chemical properties of the hydrogels. When laponite is suspended in water, it forms disc-like particles with a thickness of 1 nm, a diameter of about 25 nm, and a

G. R. Mahdavinia (✉)
Department of Chemistry, Faculty of Science, University
of Maragheh, P.O. Box: 55181-83111, Maragheh, Iran
e-mail: mahdavin@yahoo.com

A. Massoudi · A. Baghban · B. Massoumi
Department of Chemistry, Faculty of Science,
Payame Noor University, P.O. Box: 19395-3697, Tehran, Iran

negative surface charge density to form stabilizing dispersion in water [5]. A wide range of nanocomposite hydrogels derived from monomers like acrylamide [6, 7], N-isopropyl acrylamide [8], and acrylic acid [9] has been synthesized using laponite nanoclay as cross-linker or filler.

Industry is a huge source of water pollution; it produces pollutants that are extremely harmful to people and the environment. Many industries like dye, textile, paper, and plastic facilities produce considerable colored wastewater. Dyes are the type of pollutant from industry damaging the environment, which must be removed from wastewater before being discharged into the environment. Because of the stability of dyes toward light and oxidation, it is difficult to treat polluted wastewaters using conventional methods [10]. Adsorption process, an inexpensive and simple design, can be used to remove dye contaminations from aqueous environments [11]. Anionic and cationic hydrogels are a class of polymeric networks that have been widely used as adsorbents to treat wastewaters containing dye pollutions [12–14]. The electrostatic and polar interactions between dyes and hydrogels leading to hydrogel–dye complex formation show interesting and practical features. But, because these hydrogels do not possess enough strength, the introduction of nanoclays into hydrogel compositions can be considered as one of the methods to improve hydrogels physically and mechanically [15]. It has been reported that the inclusion of nanoclays into the hydrogel composition not only improves the strength of the hydrogel, but also increases the rate and dye adsorption capacity [16]. Hydrogel nanocomposites containing Na-montmorillonite [17], laponite [18], attapulgite [19], and sepiolite [20] have been synthesized and applied to remove pollutions from colored waters. Depending on the type of electronic charge of the dyes, anionic and cationic nanocomposite hydrogels can be used to remove dyes from wastewaters.

Carrageenan is a collective term for linear sulfonated polysaccharide that can be prepared by alkaline extraction from red seaweed. Non-toxicity, biodegradability, and biocompatibility of carrageenan make this biopolymer a favorable candidate in the synthesis of hydrogels. In our earlier study, we reported the synthesis of carrageenan-based hydrogel nanocomposites using Na-montmorillonite as nanoclay and methylenebisacrylamide as cross-linker [21]. In this work, we endeavored to use laponite nanoclay as a cross-linker. Carrageenan-based hydrogel nanocomposites were synthesized using solution polymerization of acrylamide monomer in the presence of laponite RD and carrageenan biopolymer. The so-obtained nanocomposites were used to remove cationic CV dye from aqueous solution. The rate of removal and kinetics of dye adsorption by nanocomposites was investigated.

## Experimental

### Materials

Kappa-Carrageenan was obtained from Condinson Co., Denmark, ammonium persulfate (APS) from Fluka and acrylamide (AAm) from Nalco Chemical Co., The Netherlands, of analytical grades, and was used as received. Laponite RD was provided by Rockwood Additive Limited (surface area: $370 \ m^2/g$, bulk density: $1,000 \ kg/m^3$, chemical composition: $SiO_2$ 59.5 %, MgO 27.5 %, $Li_2O$ 0.8 %, $Na_2O$ 2.8 %, loss on ignition: 8.2 %). All other ingredients were of analytical grade and were also used as received.

### Synthesis of nanocomposite hydrogels

Table 1 shows the reaction variables employed to synthesize the nanocomposite hydrogels. The suffixes m and n in clay$_m$ and carra$_n$ are wt % of clay and carrageenan, respectively. In general, laponite was dispersed in 30 mL of distilled water and stirred under a magnetic stirrer for 5 h. The dispersed clay solution was transferred to a 1–l reactor equipped with a mechanical stirrer. To control the reaction temperature, the reactor was placed in a water bath preset at 60 °C. Then, carrageenan was added to the solution containing clay and stirred until completion of dissolution. AAm was added into the solution and stirred for 1 h. Finally, APS (0.05 g in 2 mL of water) was added as initiator into the solution and stirred for 3 min. After this stage, the solution was transferred into a test tube (interior size: 12 mm in diameter and 160 mm long) and was kept in an oven at 60 °C for 3 days. The obtained nanocomposites were purified by their immersion in excess distilled water to extract the unreacted and sol part of the samples. The resulting hydrogel nanocomposites were dried at ambient temperature for 7 days. Afterward, the dried nanocomposites were milled and sieved for 40–60 mesh size and kept away from light and moisture.

### Swelling studies

The degree of swelling (DS) of nanocomposites was determined by immersing 0.1 g of purified nanocomposites in distilled water (200 mL) and allowing to soak for 24 h at room temperature. Then, the samples were removed from water, blotted with filter paper to remove surface water, weighed and the DS calculated using Eq. 1:

$$DS = \frac{W_s - W_d}{W_d} \qquad (1)$$

where $W_s$ and $W_d$ are the weights of the samples swollen in water and in dry state, respectively.

**Table 1** Reaction variables content to synthesis of nanocomposite hydrogels (water: 32 mL, $T$: 60 °C, AAm: 3 g, and APS: 0.05 g)

|  | Clay2.7 | Clay6.6 | Clay12.5 | Clay17.6 | Carra0 | Carra12.5 | Carra22 |
|---|---|---|---|---|---|---|---|
| Carrageenan (g) | 0.5 | 0.5 | 0.5 | 0.5 | 0 | 0.5 | 1 |
| Clay (g) | 0.1 | 0.25 | 0.5 | 0.75 | 0.5 | 0.5 | 0.5 |

## Gel content

An amount of 0.2 g of each nanocomposite was immersed in distilled water for 72 h, and then the swollen nanocomposites were filtered, dewatered with 200 mL ethanol, and dried at 70 °C for 5 h. The dried samples were weighed and the gel content (Gel %) was calculated by Eq. 2.

$$Gel\% = \frac{m}{M} \times 100 \tag{2}$$

where $m$ and $M$ designate final and initial weights of the sample, respectively.

## Water retention capacity

For measuring the water retention at ambient temperature, the swollen nanocomposites were put into syringes and centrifuged at constant rate (e.g., 4,000 rpm). The weights of the nanocomposites were recorded at suitable times to investigate the relationship between their weights and the centrifuging time.

## Adsorption of CV dye

Dye adsorption was carried out by immersing 0.05 g of nanocomposites into 50 mL of dye solution with 30 mg L$^{-1}$ of CV solution. All adsorption experiments were examined through a batch method on a stirrer with a constant speed at 120 rpm. To study the adsorption kinetics, at specified time intervals, the amount of adsorbed CV was evaluated using a UV spectrometer at $\lambda_{max} = 590$ nm. The content of adsorbed dye was calculated using the following Eq. 3:

$$q_t = \frac{(C_0 - C_t)}{m} \times V \tag{3}$$

where, $C_0$ is the initial CV concentration (mg L$^{-1}$), $C_t$ is the remaining dye concentrations in the solution at time $t$, $V$ is the volume of dye solution used (L), and $m$ is the weight of nanocomposite (g). Adsorption isotherm was carried out by separate immersion of 0.05 g of a nanocomposite into 50 mL of dye solutions with 5, 10, 15, 20, 25, 30, 40, 50, 70, 90, and 120 mg L$^{-1}$ of CV for 24 h. The equilibrium adsorption capacity of nanocomposites, $q_e$ (mg L$^{-1}$), was determined using Eq. 3. In this equation, $C_t$ and $q_t$ may be replaced with equilibrium concentration of dye in the solution ($C_e$) and equilibrium adsorption capacity ($q_e$), respectively.

The removal efficiency (RE %) of CV by nanocomposites was calculated as follows:

$$RE\% = \frac{C_0 - C_e}{C_0} \times 100 \tag{4}$$

where, $C_e$ is the remaining CV concentration in the solution.

## Instruments

Dried nanocomposite was coated with a thin layer of gold and imaged in an SEM instrument (Vega, Tescan). One-dimensional, wide angle X-ray diffraction patterns were obtained by using a Siemens D-500 X-ray diffractometer with wavelength $\lambda = 1.54$Å (Cu–Kα), at a tube voltage of 35 kV, and tube current of 30 mA. TEM Micrographs were recorded with a Philips CM10 operating at 60 kV tension.

## Results and discussions

### Synthesis and characterization

Carrageenan-based nanocomposite hydrogels were synthesized using solution polymerization. Acrylamide and laponite RD were used as monomer and nanoclay cross-linker, respectively. The polymerization was carried out using APS as initiator. APS as thermal initiator can decompose to sulfate anion radical on heating at 60 °C. Polymerization of acrylamide is initiated in the presence of sulfate anion radical. Before adding the initiator, AAm monomer was added into dispersed clay solution and allowed to stir for 1 h to diffuse into the clay layers. At the time of polymerization, the produced PAAm would be captured inside the laponite layers. The carrageenan biopolymer cannot intercalate into laponite layers because of its anionic character. But, subsequently it can be captured between PAAm and laponite networks and form a semi-IPN nanocomposite hydrogel. A simple mechanism is shown in Scheme 1.

The XRD patterns of pristine laponite RD and nanocomposites were studied at $2\theta = 2.5$–$15°$ and are illustrated in Fig. 1. According to data, the XRD profile of pristine laponite (Fig. 1a) shows a broad peak from
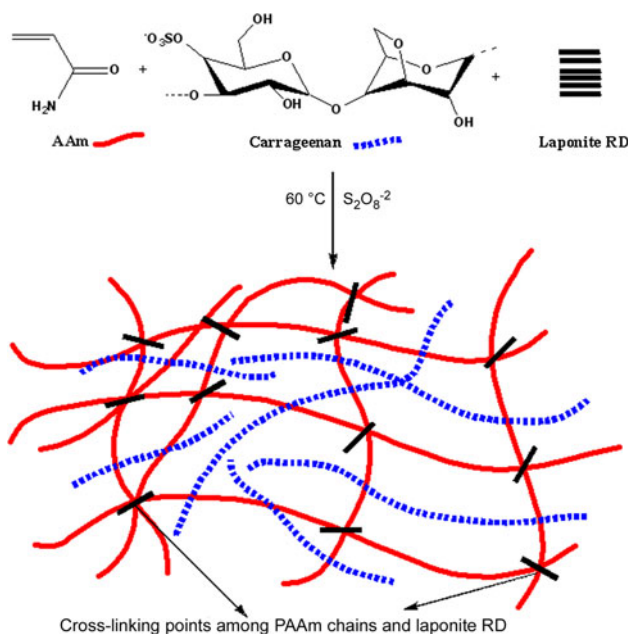
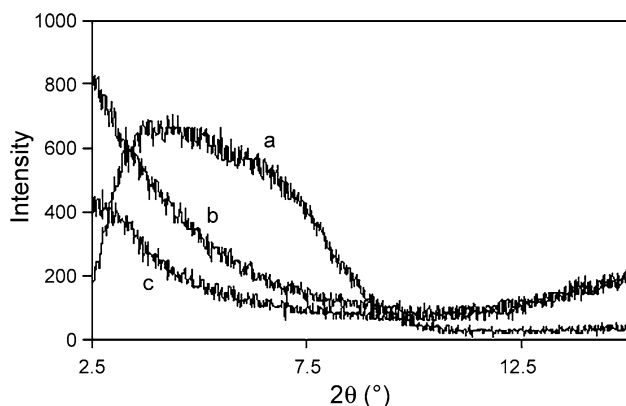Scheme 1 A simple mechanism for synthesis of carrageenan-based hydrogel nanocomposite



Fig. 2 TEM image of Clay6.6 hydrogel nanocomposite



Fig. 1 XRD patterns of: a pristine laponite RD, b Clay2.7 nanocomposite and c Clay12.5 nanocomposite

$2\theta = 2.5°$ to $2\theta = 9.1°$ with a diffraction peak at about $2\theta = 4.32°$ corresponding to the distance of clay sheets with $d$ spacing 20.4Å. Stirring of laponite for 5 h and the subsequent in situ polymerization of AAm in the presence of carrageenan biopolymer led to nanocomposite hydrogels with the XRD profiles shown in Fig. 1b, c. No diffraction peak was observed in nanocomposites and it can be concluded that the clay layers are completely exfoliated. The results indicate that the clay content up to 12.5 wt % of clay cannot influence the type of dispersion of nanoclay in nanocomposite matrix. TEM can be used to confirm the XRD results and type of clay dispersion in the polymer matrix. The TEM image of nanocomposite containing 6.6 wt % of laponite is shown in Fig. 2. The dark lines
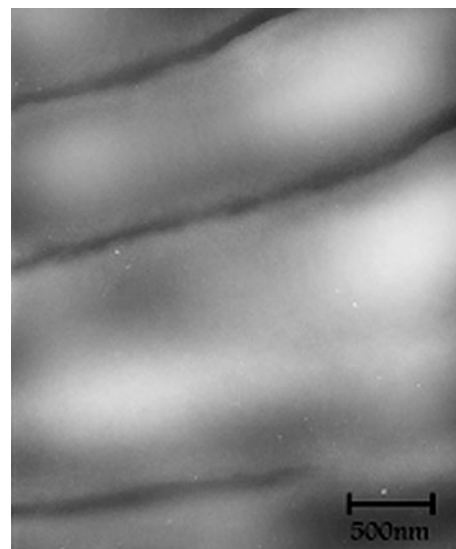
correspond to laponite layers. It is seen that laponite layers indicate that the clay layers are exfoliated due to acrylamide polymerization in the presence of laponite clay. The morphology of hydrogel microstructure is considered as one of the most important properties of nanocomposites. Figure 3 depicts the surface morphology of cross-linked clay-free hydrogel (Fig. 3a) and hydrogel nanocomposite (Fig. 3b). By inclusion of laponite as clay into the hydrogel, the surface of both conventional and nanocomposite hydrogels was obtained to be relatively smooth and similar.

Swelling of nanocomposites

The effect of laponite and carrageenan contents on the degree of swelling of nanocomposites was investigated. To study the influence of laponite on the swelling capacity, polymerization was carried out at four different clay contents, ranging from 2.7 to 17.6 wt % of laponite RD and the results are shown in Fig. 4. It may be noted that when the clay content was lower than 2.7 wt %, the gel strength of nanocomposites showed insignificant improvement. Above 17.6 wt % of nanoclay, the dispersion of laponite produced a pasty solution and it was difficult to dissolve carrageenan in the laponite dispersion. Therefore, the clay content was changed from 2.7 to 17.6 wt % in polymerization feed.

Although laponite acts as a cross-linker, the results revealed that the swelling capacity was enhanced by increasing the clay content from 2.7 to 17.6 wt % of laponite content. In the conventional hydrogels, the water absorbency is decreased as the cross-linker is increased in hydrogel composition [1]. The water absorbency of

**Fig. 3** SEM micrographs of:
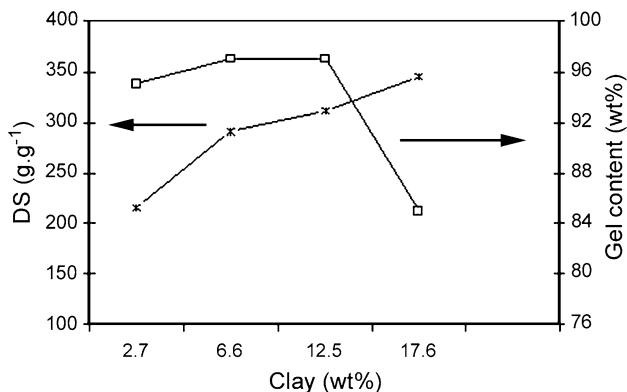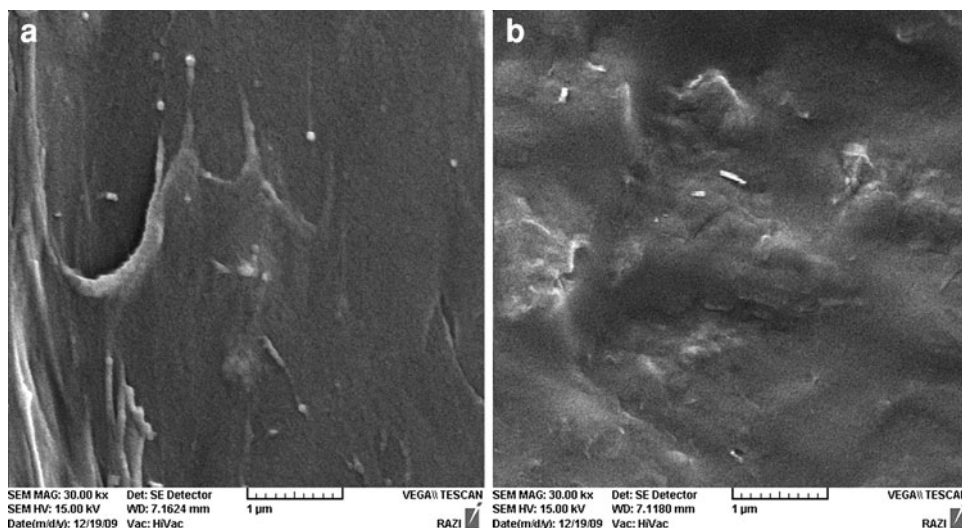**a** clay-free hydrogel and
**b** Clay12.5 nanocomposite



**Fig. 4** Influence of clay content on the degree of swelling and gel content of nanocomposites



**Fig. 5** Degree of swelling and gel content of nanocomposites as a function of carrageenan content

Clay2.7 and Clay17.6 was 216 g/g and 345 g/g, respectively. The corresponding increase in swelling could be attributed to the increase in ionic osmotic pressure of nanocomposites. This osmotic pressure is due to the mobile ions on the nanoclay particles [22]. Also, the effect of laponite amount on the gel content was studied and is shown in Fig. 4. According to the results, by varying laponite content from 2.7 to 12.5 wt %, the change in gel content of nanocomposites is not notable (95–97 wt %). Decrease in gel content beyond 12.5 wt % of laponite can be attributed to the viscosity enhancement of polymerization medium that restricts the macroradical movement, thereby decreasing the gel content.

We tried to study the swelling of nanocomposites by varying the carrageenan content. The carrageenan content was chosen to be 0, 12.5, and 22 wt % of the initial feed. The results are depicted in Fig. 5. While the water uptake capacity for hydrogel nanocomposite without carrageena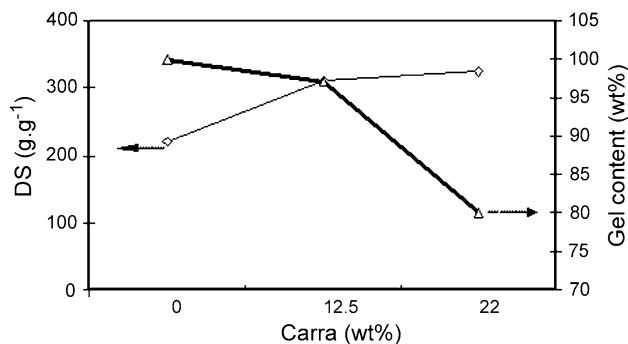n was 210 g/g, it was increased by its introduction into nanocomposites. As evident from the data, all nanocomposites containing carrageenan component have swelling capacity above 210 g/g. Carrageenan is an anionic biopolymer comprising anionic sulfonate groups. Inclusion of ionic charges into hydrogel composition not only results in anionic–anionic repulsion, but also causes increases in ionic osmotic pressure of hydrogel and subsequently its swelling capacity [23]. A similar result for carrageenan-based nanocomposite was obtained in our previous work using sodium montmorillonite nanoclay [21]. The effect of carrageenan on the gel content of nanocomposites is indicated in Fig. 5. The gel content for Carra22 was 80 wt %. This decrease in gel content can be described as the above stated for the laponite variable.

Water retention capacity under centrifugation

In this part of the work, we used a centrifuge to demonstrate the water retention capacity of the nanocomposites. Swollen nanocomposites were centrifuged and the influence of laponite content on water retention capacity was
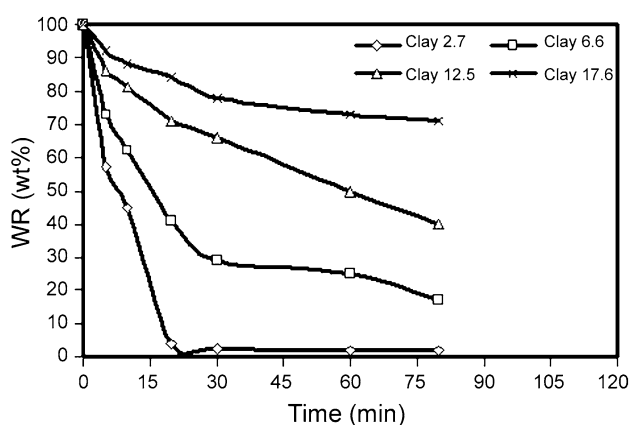
**Fig. 6** Water retention of nanocomposites as a function of clay content using centrifuge technique
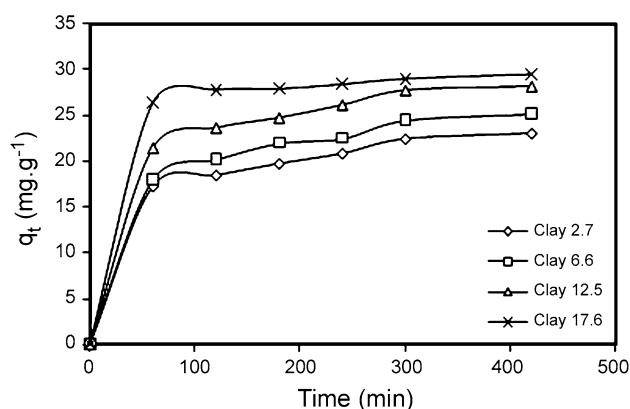


**Fig. 7** Dynamic adsorption kinetic of nanocomposites as a function of clay content (0.05 g of samples, 50 mL of 30 mg L$^{-1}$ of CV dye, $T$ 25 °C)

studied. The results are indicated in Fig. 6. As it is clear from the data, the laponite content affects the water retention of nanocomposites. By increasing the clay content in the nanocomposite composition, water retention was increased. In contrast, the rate of water loss is decreased as the clay content is increased in nanocomposite composition. In fact, the polymer chains are not only inserted into clay layers, but, by increases in clay contents, there would also be more extensive interactions of polymer chains with the surface of the clay, which restrict the mobility of polymer chains [24]. A restricted mobility of chains can cause retention of water in nanocomposites. During 30 min, the water loss for Clay17.6 and Clay2.7 is found to be 12 and 98 %, respectively.

Dye adsorption study

Contact time, initial dye concentration, and properties of adsorbents are three important variables that can influence

the adsorption properties of adsorbents [25]. Among them, contact time is an important parameter. If the contact time is not sufficient, only a fraction of dye will be removed by adsorbents. The study of the contact time can reveal the rate of removal of dye as well as the equilibrium adsorption time. The composition of adsorbents is another important factor that may affect the adsorbing capacity. Cationic dyes containing ammonium groups can adsorb onto adsorbent containing anionic centers through electrostatic interactions. So, the content of anionic groups of the adsorbents is an effective parameter that can influence the dye adsorption speed and capacity.

Clay and carrageenan contents in relation to dye adsorption

Dye adsorption speed of nanocomposites as a function of clay content is shown in Fig. 7. All samples were placed in contact with solutions containing 30 mg L$^{-1}$ of CV at specific time intervals, and the adsorption capacity was recorded. As can be seen from this figure, the clay content easily affects the rate of dye removal. In fact, dye adsorption speed is enhanced as the clay content in the nanocomposite composition is increased. Table 2 represents the dye adsorption capacity of nanocomposites after 120 min. At this time, while the removal efficiency is 93 % for Clay17.6, it is only 62.5 % for nanocomposite with the lowest clay content. The data show that the rate of dye removal is increased by higher clay content. By introducing the laponite into hydrogel, because of negative surface of the clay, the negative charge density would be increased. The higher the content of laponite in the nanocomposite, the higher negative charges would result in the hydrogel [26]. According to Table 2, the RE % of dye by nanocomposites is in agreement with the rate of dye adsorption and increase in clay content is enhanced dye removal efficiency.

To study the effect of carrageenan content on the speed of dye adsorption of nanocomposites, we synthesized nanocomposites containing various amounts of carrageenan while the laponite content was the same. The results are illustrated in Fig. 8. There are anionic sulfonate groups on the carrageenan backbones. It was our expectation that like laponite content,

**Table 2** Dye removal efficiency of nanocomposites containing different contents of clay (0.05 g of nanocomposites in 50 mL of 30 mg L$^{-1}$ of CV dye)

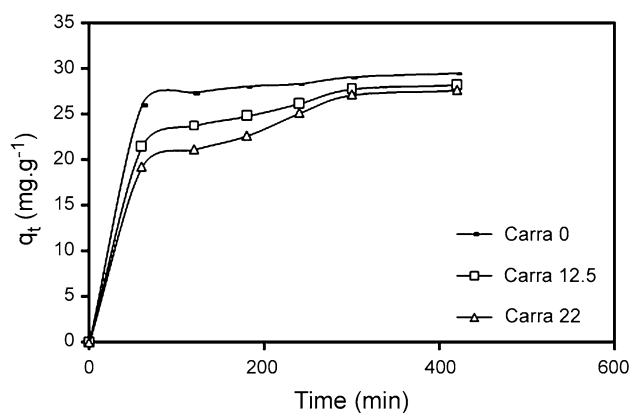|  | Removal efficiency after 120 min (%) | RE (%) |
|---|---|---|
| Clay2.7 | 62.5 | 76.5 |
| Clay6.6 | 64.9 | 81.9 |
| Clay12.5 | 81.2 | 95.6 |
| Clay17.6 | 93 | 98.6 |

**Fig. 8** Dynamic adsorption kinetic of nanocomposites as a function of carrageenan content (0.05 g of samples, 50 mL of 30 mg $L^{-1}$ of CV dye, $T$ 25 °C)

**Table 3** Dye removal efficiency of nanocomposites containing different contents of carrageenan (0.05 g of nanocomposites in 50 mL of 30 mg $L^{-1}$ of CV dye)

|  | Removal content after 120 min (%) | RE (%) |
|---|---|---|
| Carra0 | 91.6 | 99.1 |
| Carra12.5 | 84.1 | 96.2 |
| Carra22 | 70 | 92.1 |
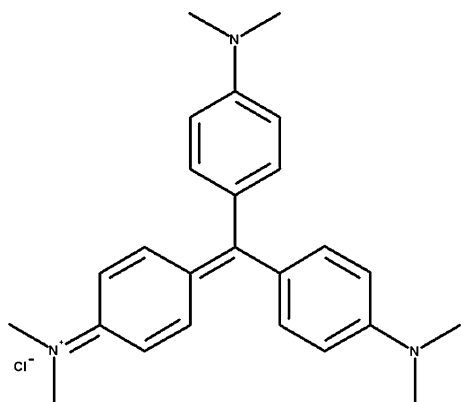


**Scheme 2** Structure of crystal violet dye

the speed of dye adsorption can increase by a higher amount of carrageenan in the nanocomposite composition. As the results demonstrate, with an increase in the amount of carrageenan, the rate of dye adsorption is decreased. According to Table 3, after 120 min, while the removal efficiency is 91.6 % for nanocomposite with no carrageenan present, it is only 70 % for nanocomposite with the highest carrageenan content. These data revealed that the rate of dye removal is decreased by increases in carrageenan content. Also, the RE % of dye onto nanocomposites decreased as the carrageenan content increased. The low adsorption capacity and low rate of adsorption of nanocomposite with high content of

carrageenan may be attributed to high hydrophilic property of carrageenan. This property of carrageenan hinders the ease of cationic dye approach toward large hydrophobic segments (Scheme 2).

Adsorption kinetics

Adsorption kinetics represents the pollutant adsorption rate, which dominates the time of adsorbate adsorption at the solid–liquid surface [19]. In fact, kinetic of adsorption is one of the most important factors for estimating the adsorption efficiency. Pseudo-first-order and pseudo-second-order kinetic models were examined to obtain rate constant and equilibrium adsorption capacity for all nanocomposite samples. So, kinetic data were analyzed by using the following equations [27].

Pseudo first order

$$Ln\,(q_e - q_t) = Ln\,q_e - k_1 t \qquad (5)$$

where $q_e$ and $q_t$ (mg g$^{-1}$) are the amounts of adsorbed dye on the nanocomposites at equilibrium and at time $t$, respectively. $k_1$ (min$^{-1}$) presents the rate constant of first-order adsorption.
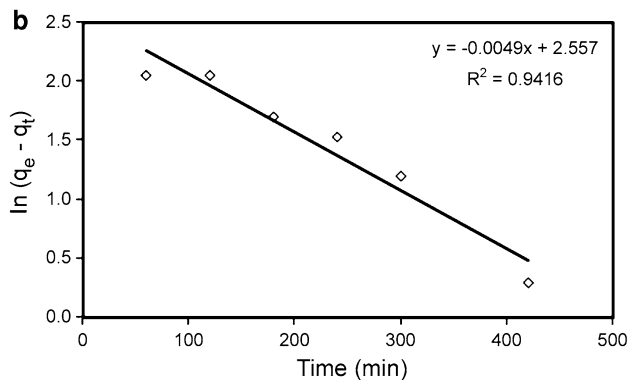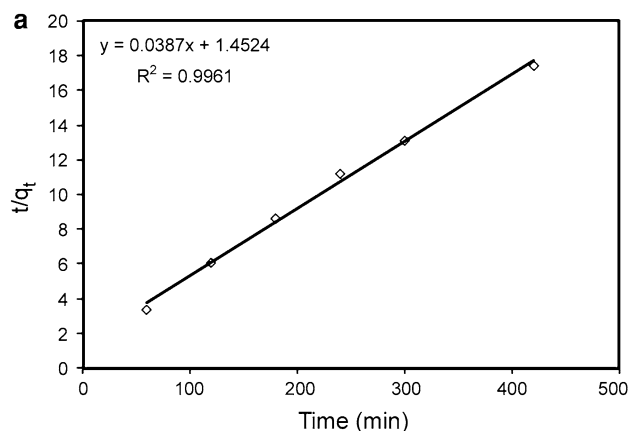


**Fig. 9** Relationship between **a** $\frac{t}{q_t}$ in Pseudo-second-order equation and **b** $Ln\,(q_e - q_t)$ in pseudo-first-order equation versus contact time for Clay6.6 nanocomposite

**Table 4** Parameters and correlation coefficient of pseudo-second-order and pseudo-first-order kinetics for nanocomposites

| | First-order kinetics | | | | Second-order kinetics | | | |
|---|---|---|---|---|---|---|---|---|
| | $K_1 \times 10^3$ (min$^{-1}$) | $R^2$ | $q_e$, Exp. (mg g − 1) | $q_e$, Theor. (mg g − 1) | $K_2 \times 10^3$ (g mg$^{-1}$ min$^{-1}$) | $R^2$ | $q_e$, Exp. (mg g$^{-1}$) | $q_e$, Theor. (mg g$^{-1}$) |
| Carra0 | 5.3 | 0.968 | 29.4 | 5.2 | 2.51 | 0.994 | 29.4 | 30.4 |
| Carra22 | 5.9 | 0.965 | 27.6 | 16.2 | 0.65 | 0.975 | 27.6 | 28.1 |
| Clay2.7 | 8.3 | 0.972 | 23.1 | 11.7 | 1.205 | 0.984 | 23.1 | 24.6 |
| Clay6.6 | 4.9 | 0.941 | 26.2 | 12.67 | 1.034 | 0.996 | 26.2 | 25.8 |
| Clay12.5 (Carra12.5) | 9.35 | 0.949 | 28.7 | 14.9 | 1.12 | 0.999 | 28.7 | 30.15 |
| Clay17.6 | 7.8 | 0.964 | 29.6 | 3.8 | 3.78 | 0.998 | 29.6 | 29.8 |
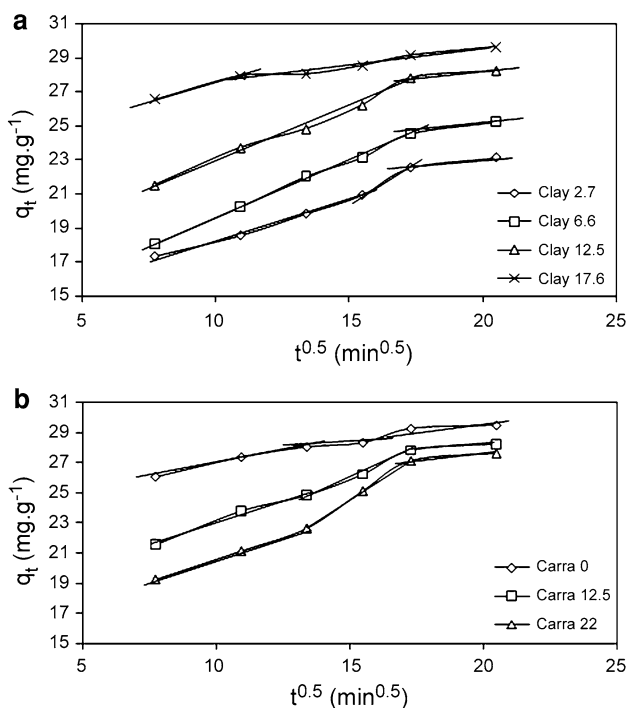


**Fig. 10** Intraparticle diffusion kinetics of CV dye onto nanocomposites: **a** clay series and **b** carrageenan series

Pseudo second order

$$\frac{t}{q_t} = \frac{1}{k_2 q_e^2} + \frac{t}{q_e} \tag{6}$$

where $k_2$ (g mg$^{-1}$ min$^{-1}$) is rate constant of second-order adsorption and $q_e$ is the theoretical adsorbed dye (mg g$^{-1}$) that can be calculated from pseudo second order.

To obtain model calculations, we can plot $Ln (q_e - q_t)$ against $t$ for pseudo first order and $\frac{t}{q_t}$ against $t$ for pseudo second order. For example, the curves for Clay6.6 nanocomposite are illustrated in Fig. 9a, b. Model calculations for all nanocomposites are given in Table 4. It was found that the plotting of $\frac{t}{q_t}$ against t gives a straight line with a

high correlation coefficient ($R^2 > 0.99$), and it can be concluded that adsorption kinetics of dye by all nanocomposites has the best fitting to the pseudo second order. As can be seen from the data, according to pseudo-second-order kinetics, the experimental and theoretical equilibrium adsorption capacities of nanocomposites are in agreement. Considering the $k_2$ values, the adsorption rate constant of carrageenan-free nanocomposite is $2.51 \times 10^{-3}$ g mg$^{-1}$ min$^{-1}$ and it decreases for nanocomposites including carrageenan component. This finding is consistent with the experimental data of adsorption rates by varying carrageenan content (Fig. 8).

The adsorption of adsorbate onto the adsorbent can take place through several steps. The steps may be considered as film diffusion, pore diffusion, surface diffusion, and adsorption on the pore surface [20]. In fact, under sufficient speed of stirring, intraparticular diffusion/transport process are the rate-limiting steps of adsorption kinetics [19]. The possibility of intraparticle diffusion can be explored according to Eq. 7:

$$q_t = k_{id} t^{0.5} + C \tag{7}$$

where $q_t$ is the amount of dye adsorbed at time $t$, $C$ is the intercept, and $k_{id}$ is the intraparticular diffusion rate constant (mg min$^{0.5}$/g).

According to Eq. 7, by plotting $q_t$ versus $t^{0.5}$, a straight line suggests that the intraparticle diffusion is the rate-limiting step. As can be seen from Fig. 10, the diffusion plot of CV onto nanocomposites is multi-linear containing two or three linear parts. The linear segments do not pass through the origin, indicating that the intraparticle diffusion is not the only rate-limiting step. The first linear segments show that the mass transfer controlling may be due to boundary layer effect [21]. To determine the exact mechanism of adsorption, the experimental data are analyzed according to Boyd's model [22]:

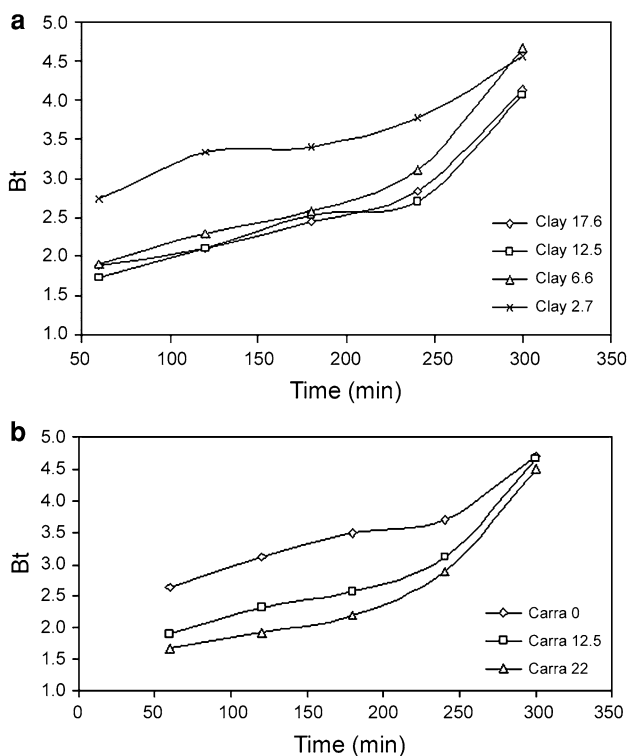$$F = 1 - \frac{6}{\pi^2} \exp(-Bt) \tag{8}$$

Fig. 11 Boyd plot for sorption of CV dye onto nanocomposites:
**a** clay series and **b** carrageenan series

where $F$ $(F = \frac{q_t}{q_e})$ is the fractional attainment of equilibrium at different times, $t$, and $Bt$ is a mathematical function of $F$. The value of $Bt$ can be calculated according to Eq. 9:

$$Bt = -0.4977 - \ln(1 - F). \tag{9}$$

The value of $Bt$ can be calculated from $F$ values at each specific time. The Boyd plot can be achieved by $Bt$ versus $t$. A straight line passing through the origin is indicative of sorption process governed by intraparticle diffusion mechanism. Non-linear plot shows that the adsorption is dominated by film diffusion [22]. Figure 11 illustrates the plotting of $Bt$ versus $t$. According to Fig. 11, the plot is a straight line at the beginning and then deviates from the origin. In can be concluded that at first adsorption obeys the layer boundary effect and then the intraparticle diffusion dominates the mechanism of adsorption [22].

Adsorption isotherms

The adsorption of CV onto nanocomposites as a function of initial dye concentration was studied by immersing 0.05 g of selected nanocomposites into dye solution with concentrations ranging from 5 to 120 mg L$^{-1}$. Initially, as the concentration of CV in solution was increased, the amount of adsorbed dye by nanocomposites increased and at high
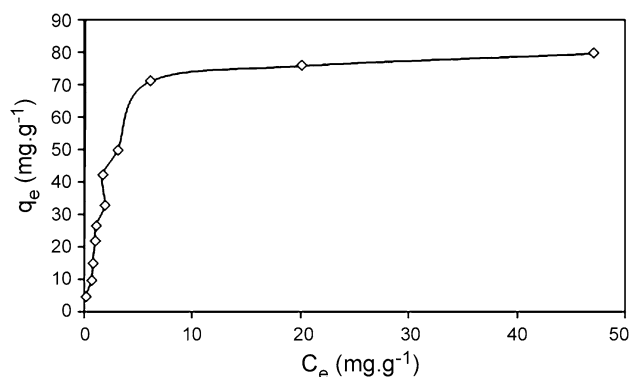


Fig. 12 Adsorption isotherm profile for the adsorption of CV by Clay17.6 nanocomposite
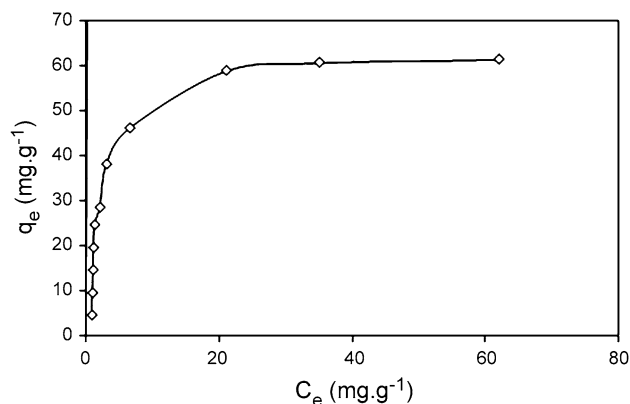


Fig. 13 Adsorption isotherm profile for the adsorption of CV by Carra22 nanocomposite

concentration of CV it began to level off. This indicates that the adsorbent gradually becomes saturated and approaches a state of maximum adsorption. This observation can be attributed to the increase in momentum of the mass transfer as the initial dye concentration is increased [28]. In fact, when the nanocomposites reach a saturated state, there are no more vacant adsorption sites and the adsorption capacity remains constant. Figures 12 and 13 show the equilibrium adsorption values onto Clay17.6 and Carra22 nanocomposites, respectively.

The interactions between adsorbate and adsorbent until a state of equilibrium can be studied using adsorption isotherms. The adsorption isotherms describe the optimized adsorption system as well as the effectiveness of adsorbents [19]. In fact, it is important to investigate an optimum isotherm model indicating the CV adsorption system onto nanocomposite hydrogels. The practical data were fitted to the Langmuir and Freundlich models. In the Langmuir adsorption model, adsorption of adsorbate takes place at specific homogeneous sites within the adsorbent and is valid for monolayer adsorption onto adsorbents. The

**Table 5** Parameters, correlation coefficient, and experimental $q_e$ of nanocomposites according to Langmuir and Freundlich isotherms

| Isotherms | Parameters | Samples | | | | | |
|---|---|---|---|---|---|---|---|
| | | Clay2.7 | Clay6.6 | Clay12.5 (Carra12.5) | Clay17.6 | Carra0 | Carra22 |
| Freundlich model | $n$ (g L$^{-1}$) | 2.15 | 2.48 | 2.32 | 2.19 | 2.15 | 2.28 |
| | $K_f$ (mg g$^{-1}$) | 9.8 | 12.85 | 14.3 | 18.5 | 21.1 | 13.9 |
| | $R^2$ | 0.885 | 0.771 | 0.648 | 0.71 | 0.5867 | 0.685 |
| Langmuir model | $q_m$ (mg g$^{-1}$) | 47.1 | 55.6 | 67.3 | 80.2 | 77.1 | 61.9 |
| | $b$ (L mg$^{-1}$) | 0.18 | 0.32 | 0.27 | 0.41 | 0.51 | 0.35 |
| | $R^2$ | 0.991 | 0.995 | 0.991 | 0.956 | 0.962 | 0.986 |
| $q_e$ (Exp.) (mg g$^{-1}$) | | 46.9 | 53.8 | 63.2 | 74 | 79.8 | 61.2 |

expression of the applied Langmuir model is given by Eq. 10 [11]:

$$\frac{C_e}{q_e} = \frac{C_e}{q_m} + \frac{1}{q_m b} \quad (10)$$

where $C_e$ is the equilibrium dye concentration in the solution (mg L$^{-1}$), $b$ is the Langmuir adsorption constant (L mg$^{-1}$), and $q_m$ is the theoretical maximum adsorption capacity (mg g$^{-1}$). $q_m$ and $b$ can be calculated from the slope and intercept of a linear plot of $\frac{C_e}{q_e}$ versus $C_e$, respectively.

In the Freundlich model, the adsorption of adsorbate occurs on a heterogeneous surface by multilayer sorption and the adsorption capacity can increase with an increase in adsorbate concentration [29]. Freundlich isotherm is represented by the following equation:

$$Ln\, q_e = Ln\, k_f + \frac{1}{n} Ln\, C_e \quad (11)$$

where $K_f$ is the equilibrium adsorption coefficient (L g$^{-1}$) and $1/n$ is the empirical constant. The $K_f$ and $n$ values for nanocomposites can be achieved from the intercept and the slope of $Ln\, q_e$ against $Ln\, C_e$. All the expressions in Langmuir and Freundlich equations and equilibrated dye adsorption of all nanocomposites were calculated according to experimental data and summarized in Table 5. In accordance with the high correlation coefficient in Langmuir equation ($R^2 > 0.96$), Langmuir isotherm is the best fit of experimental data compared to the Freundlich model. In addition, as can be seen from Langmuir data, the theoretical maximum adsorption capacity ($q_m$) is consistent with the experimental data ($q_e$). Considering the results, it is concluded that the adsorption of CV onto nanocomposites takes place through monolayer adsorption. Maximum adsorption capacity was obtained for carrageenan-free nanocomposite with 79.8 mg g$^{-1}$ of CV adsorbed onto Carra0 nanocomposite.

## Conclusion

Novel nanocomposite hydrogels, based on carrageenan and cross-linked polyacrylamide by inorganic laponite RD nanoclay, were synthesized by solution polymerization. A summary of the results of this work is as below.

- The XRD study revealed that the dispersion of laponite in nanocomposites matrix is homogeneous and of the exfoliate type. TEM study confirmed the XRD results.
- Laponite RD was successfully used to synthesize carrageenan-based hydrogel nanocomposites without using organic cross-linker. While the laponite acted as a cross-linker, the water absorbency of nanocomposites increased as the laponite content also increased.
- The water retention study of nanocomposites using the centrifuge technique depicted that the rate of water loss decreased by increasing laponite content in nanocomposite.
- While the speed of dye adsorption onto nanocomposites was enhanced by increasing the clay content, it was decreased as the carrageenan content was increased in nanocomposite composition.
- The results showed that the pseudo-second-order adsorption kinetics was predominant in the adsorption of CV onto nanocomposites.
- Langmuir model was obtained as the best model for the adsorption of CV onto nanocomposites.

## References

1. Chang C, Zhang L (2011) Cellulose-based hydrogels: present status and application prospects. Carbohyd Polym 84:40–53
2. Haraguchi K (2007) Nanocomposite hydrogels. Curr Opin Solid St M 11:47–54
3. Haraguchi K, Takehisa T (2002) Nanocomposite hydrogels: a unique organic–inorganic network structure with extraordinary mechanical, optical, and swelling/de-swelling properties. Adv Mater 14:1120–1124
4. Haraguchi K, Takehisa T, Fan S (2002) Effects of clay content on the properties of nanocomposite hydrogels composed of poly (N-isopropylacrylamide) and clay. Macromolecules 35:10162–10171
5. Can V, Abdurrahmanoglu S, Okay O (2007) Unusual swelling behavior of polymer–clay nanocomposite hydrogels. Polymer 48:5016–5023

6. Li P, Kim NH, Siddaramaiah, Lee JH (2009) Swelling behavior of polyacrylamide/laponite clay nanocomposite hydrogels: pH-sensitive property. Compos Part B Eng 40:275–283

7. Okay O, Oppermann W (2007) Polyacrylamide–clay nanocomposite hydrogels: rheological and light scattering characterization. Macromolecules 40:3378–3387

8. Siddharthya KM, Ronald AS (2008) Introduction of pH-sensitivity into mechanically strong nanoclay composite hydrogels based on N-isopropylacrylamide. J Polym Sci Polym Chem 46:6630–6640

9. Li P, Kim NH, Hui D, Rhee KY, Lee JH (2009) Improved mechanical and swelling behavior of the composite hydrogels prepared by ionic monomer and acid-activated laponite. Appl Clay Sci 46:414–417

10. Annadurai G, Juang RS, Lee DJ (2002) Use of cellulose-based wastes for adsorption of dyes from aqueous solutions. J Hazard Mater B 92:263–274

11. Ahmad R, Kumar R (2011) Adsorption of amaranth dye onto alumina reinforced polystyrene. Clean Soil Air Water 39:74–82

12. Xu D, Hein S, Loo LS, Wang K (2001) Modified chitosan hydrogels for the removal of acid dyes at high pH: modification and regeneration. Ind Eng Chem Res 50:6343–6346

13. Solpan D, Duran S, Torun M (2007) Removal of cationic dyes by poly(acrylamide-co-acrylic acid) hydrogels in aqueous solutions. Radiat Phys Chem 77:447–452

14. Karadag E, Saraydin D, Guven O (1998) Removal of some cationic dyes from aquatic solutions by acrylamide/itaconic acid hydrogels. Water Air Soil Pollut 106:369–378

15. Pissis P (2006) In: Blitz JP, Gunko VM (eds) Surface chemistry biomedical and environmental science. Springer, Netherlands, pp 229–240

16. Liu P, Zhang L (2007) Adsorption of dyes from aqueous solutions or suspensions with clay nano-adsorbents. Sep Purif Technol 58:32–39

17. Dalaran M, Emik S, Guclu G, Iyim TB, Ozgumus S (2009) Removal of acidic dye from aqueous solutions using poly (DMAEMA–AMPS–HEMA) terpolymer/MMT nanocomposite hydrogels. Polym Bull 63:159–171

18. Li P, Siddaramaiah Kim NH, Yoo GH, Lee JH (2009) Poly(acrylamide/laponite) nanocomposite hydrogels: swelling and cationic dye adsorption properties. J Appl Polym Sci 111:1786–1798

19. Liu Y, Wang W, Jin Y, Wang A (2011) Adsorption behavior of methylene blue from aqueous solution by the hydrogel composites based on attapulgite. Sep Purif Technol 46:858–868

20. Ekici S, Isikver Y, Saraydın D (2006) Poly(acrylamide-sepiolite) composite hydrogels: preparation, swelling and dye adsorption properties. Polym Bull 57:231–241

21. Mahdavinia GR, Bagheri-Marandi G, Kiani G, Pourjavadi A (2010) Semi-IPN carrageenan-based nanocomposite hydrogels: synthesis and swelling behavior. J Appl Polym Sci 118:2989–2997

22. Li A, Zhang J, Wang A (2007) Preparation and slow-release property of a poly(acrylic acid)/attapulgite/sodium humate superabsorbent composite. J Appl Polym Sci 103:37–45

23. Mahdavinia GR, Pourjavadi A, Zohuriaan-Mehr MJ (2004) Modified chitosan. 4. Superabsorbent hydrogels from polyacrylic grafted chitosan with salt- and pH-responsiveness properties. Eur Polym J 40:1399–1407

24. Pourjavadi A, Kheirabadi M, Zohuriaan-Mehr MJ, Kabiri K (2009) Anti-polyelectrolyte superabsorbing nanocomposites: synthesis and properties. J Appl Polym Sci 114:3542–3547

25. Kasguz H, Durmus A (2008) Dye removal by a novel hydrogel–clay nanocomposite with enhanced swelling properties. Polym Adv Thenol 19:838–845

26. Dalaran M, Emik S, Guclu G, Iyim TB, Ozgumus S (2011) Study on a novel polyampholyte nanocomposite superabsorbent hydrogels: synthesis, characterization and investigation of removal of indigo carmine from aqueous solution. Desalination 279:170–182

27. Saber-Samandari S, Gazi M, Yilmaz E (2012) UV-induced synthesis of chitosan-g-polyacrylamide semi-IPN superabsorbent hydrogels. Polym Bull 68:1623–1639

28. Hameed BH, Din ATM, Ahmad AL (2007) Adsorption of methylene blue onto bamboo-based activated carbon: kinetics and equilibrium studies. J Hazard Mater 141:819–825

29. Abdel-Halim ES, Al-Deyab SS (2011) Hydrogels from crosslinked PAAm/guar gum graft copolymer for sorption hexavalent chromium ion. Carbohyd Polym 86:1306–1312